Comparison of the Hemolytic Activity and Solution Structures of Two Snake Venom Cardiotoxin Analogues Which Only Differ in Their N-Terminal Amino Acid[†,‡]

Jye-Yuan Jang, Thallampuranam Krishnaswamy S. Kumar, Gururnathan Jayaraman, Pey-Wen Yang, and Chin Yu*

Department of Chemistry, National Tsing Hua University, Hsinchu, Taiwan, ROC

Received May 12, 1997; Revised Manuscript Received September 24, 1997[⊗]

ABSTRACT: Cardiotoxin analogues IV (CTX IV) and II (CTX II) isolated from the venom of Taiwan Cobra (*Naja naja atra*) differ in their amino acid sequence by a single amino acid at the N-terminal end. Leucine at the N-terminal end in CTX II is replaced by arginine in CTX IV. CTX IV is an unique snake venom cardiotoxin as it is the only cardiotoxin isoform known so far which possesses a positively charged residue at the N-terminal amino acid. All other cardiotoxins have a hydrophobic amino acid (leucine or isoleucine) at their N-terminal end. The aim of the present study is to understand the effect(s) of the presence of a cationic residue on the structure and functional properties of cardiotoxin(s). Comparison of the hemolytic activities of CTX IV and CTX II shows that lytic activity of the former is at least twice as that shown by the latter. Comparison of the solution structures of CTX IV and CTX II using two-dimensional NMR spectroscopy and dynamical simulated annealing technique reveals that the backbone fold of both the toxin isoforms is almost similar. The secondary structural elements in these two cardiotoxin isoforms consist of long, triple-stranded, as well as short, double-stranded, antiparallel β-sheets. Thermal denaturation experiments showed that the structure of CTX IV is more stable than that of CTX II. Critical analysis of the three-dimensional structures of CTX IV and CTX II reveals the presence of a "cationic" cluster comprising of positively charged residues on the concave side of the CTX IV molecule. Similar clusters consisting of positively charged residues are not found in CTX II. The differential erythrocyte lytic activities of these two cardiotoxins are attributed to the difference(s) in the distribution of the positively charged residues in their three-dimensional structures.

Snake venom cardiotoxins are small molecular mass (6.5−7 kDa), highly basic proteins cross-linked by four disulfide bridges (Kumar *et al*., 1996a; Yu *et al*., 1994). This class of toxins (cardiotoxins) are found only in the species of *Naja* (the cobras) and *Hemachatus* (the ringhals) (Dufton & Hider, 1991). Interestingly, cardiotoxins exhibit a wide variety of biological activities which include hemolysis, cytotoxicity, depolarization of membranes of excitable cells, membrane fusion, selective killing of certain type of tumour cells, inhibition of protein kinase C activity, and muscle contraction (Kumar *et al*., 1996a).

The amino acid sequences of cardiotoxins exhibit more than 90% homology (Brackenridge & Dufton, 1987). Crystal and solution structures of few snake venom cardiotoxin (Bhaskaran *et al*., 1994b; 1994c; Jahnke *et al*., 1994; Gilquin *et al*., 1993; O'Connell *et al*., 1993) and neurotoxin (Bhaskaran *et al*., 1994a; Yu *et al*., 1993; Peng *et al*., 1997) analogues have been recently reported. Cardiotoxins isolated from different venom sources possess very similar backbone folding. These toxins are all β-sheet proteins with no helical segments. Interestingly, despite the similarities in the backbone architecture, cardiotoxin analogues isolated from the same venom source show significant differences in their biological activities (Kumar *et al*., 1996a). The differences in the biological activity among the various cardiotoxin isoforms obtained from the same venom source are believed to arise due to subtle variations in their three-dimensional structures (Dufton & Hider, 1991). In pursuit of the goal of understanding the structural basis for biological activity variations among the cardiotoxin analogues, we compare the structural and functional properties of two cardiotoxin isoforms, cardiotoxin II (CTX II) and cardiotoxin IV (CTX IV), isolated from the venom of Taiwan Cobra (*Naja naja atra*).

The amino acid sequence of CTX IV from the Taiwan Cobra (*N. naja atra*) is unique. Among the 50 odd cardiotoxins whose amino acid sequences are known, CTX IV is the only cardiotoxin isoform wherein the N-terminal amino acid is arginine (Dufton & Hider, 1991). The N-terminal residue of all other cardiotoxins is either leucine or isoleucine. It would be interesting to understand the effect(s) on the structure and function due to the presence of a positively charged residue (in CTX IV) instead of a hydrophobic amino acid (as in all other cardiotoxin analogues) at the N-terminal end. In this context, cardiotoxin analogue II (CTX II) isolated from the same snake venom source (*N. naja atra*) is an ideal choice. CTX IV and CTX II are identical to each other in their amino acid sequence,

[†] This work is supported by the Taiwan National Science Council (NSC 86-2113-M007-001 and NSC 86-2113-M007-003) and the Dr. C. S. Tsou Memorial Medical Research Advancement Foundation (VGHTH 86-0112) grants.

[‡] The atomic coordinates and structure factors of CTX II (filenames 1CRE and 1CRF) and CTX IV (filenames 1KBS and 1KBT) have been deposited in the Protein Data Bank, Brookhaven National Laboratory, Upton, NY.

* Author to whom all correspondence should be addressed. Fax: 886-35-711082. E-mail: cyu@chem.nthu.edu.tw.

[⊗] Abstract published in *Advance ACS Abstracts,* November 1, 1997.

S0006-2960(97)01107-0 CCC: $14.00

and they differ only in the amino acid at the N-terminal end. In CTX II, the N-terminal amino acid is leucine while in CTX IV it is arginine (Chiou *et al*., 1995).

The results obtained in the present study clearly demonstrate that the presence of a cationic residue such as arginine in CTX IV at the N-terminal markedly enhances its hemolytic activity. The increase in the hemolytic activity of CTX IV is rationalized by comparing the solution structures of CTX II and CTX IV.

MATERIALS AND METHODS

CTX II and CTX IV were prepared as per the procedure reported by Yang *et al*. The toxin samples were further purified by reverse-phase (C_{18}) HPLC. Anilino-naphthalene-8-sulfonate (ANS) magnesium^{2+} salt was purchased from Sigma Chemical Co. All other chemicals used were of high quality analytical grade. All experiments, unless and otherwise stated, have been carried out at room temperature. For the hemolytic activity experiments, reduced and denatured CTX (CTX II and CTX IV) samples were prepared by dissolving appropriate amounts of the toxins in 0.1 M Tris-HCl (pH 8.7), containing 8 M urea and 0.15% β-mercaptoethanol.

Hemolytic Activity. The hemolytic activity of CTX II and CTX IV was tested on erythrocytes derived from human blood per the method reported earlier (Kumar *et al*., 1996b). All measurements were carried out with appropriate controls. The percentage hemolytic activity of the cardiotoxins was calculated by assuming the lysis of erythrocytes by water as 100%. Hemolytic assay for the denatured and reduced CTX (CTX II and CTX IV) samples were also carried out under identical conditions as adopted for the native toxins.

Circular Dichroism. All CD spectra were recorded on a J-720 spectropolarimeter. The spectrometer was calibrated with ammonium *d*-10-camphorsulfonate. All measurements were made using 0.2 mm and 1 mm cells. The concentration(s) of the protein samples were estimated based on the molar extinction coefficient of the toxins at 280 nm. Necessary background corrections were made in all spectra. The protein samples were prepared in 5 mM acetate buffer (pH 3.0).

Anilinonaphthalene Binding Studies. ANS binding studies were carried out on a Hitachi F-4500 spectrofluorimeter. Appropriate volumes of 400 μM ANS and 20 μM CTX (CTX II and CTX IV) were mixed, and the fluorescence spectra were recorded between 450 and 600 nm using an excitation wavelength of 400 nm. Appropriate background corrections were made in all spectra. The protein samples were prepared in 5 mM acetate buffer (pH 3.0).

NMR Spectroscopy. Sample preparation: CTX II and CTX IV samples for the NMR experiments were prepared in H_2O(90%)/D_2O(10%) under identical conditions (4 mM, pH = 3.0, 20 °C). To achieve varied conditions of exchange of amide protons in the NMR experiments, the toxin samples (CTX II and CTX IV) were prepared in different ways (Bhaskaran *et al*., 1994b). All NMR data was acquired on a Bruker DMX-600 MHz spectrometer and processed on a Silicon Graphics Indigo II workstation using the UXNMR software. The two-dimensional homonuclear experiments

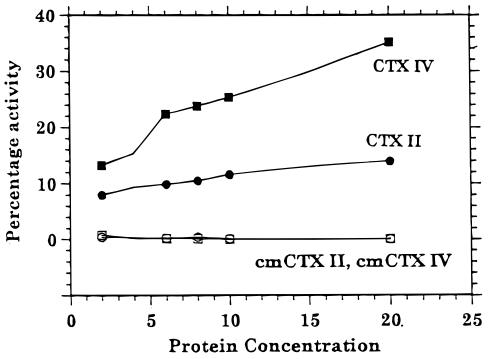

FIGURE 1: The dosage dependent hemolytic assay of CTX II and CTX IV. cmCTXII and cmCTX IV represent the *S*-carboxymethylated derivatives of CTX II and CTX IV, respectively.

carried out were DQF-COSY[1] (Rance *et al*., 1983), DQ-COSY (Wagner & Zuiderweg, 1983), TOCSY (Bax & Davies, 1985), and water-gated NOESY (Piotto *et al*., 1992). All the spectra were obtained with 2048 complex data points in t_2 (detection period) and 512 points in t_1 (evolution period) with a spectral width of 7508 Hz. The spectral data were processed and analyzed using conventional methods. Structure calculation of CTX II and CTX IV was performed using random/dynamical simulated annealing methods (Nilges *et al*., 1988), as per the software X-PLOR (Brunger, 1992). The protocol for structure determination used in this study was similar to those used in our earlier structure determination studies (Bhaskaran *et al*., 1994b; Peng *et al*., 1997).

Thermal Denaturation. Thermal denaturation of CTX II and CTX IV was followed by monitoring the mean residue ellipticity at either 213 nm or 270 nm using Jasco J720 spectropolarimeter interfaced to a Neslab RTE-110 circulating water bath. A cylindrical 2 mm water-jacketed cuvette obtained from Jasco was used for all experiments in the far-UV region, and the protein concentration used was 80 μM. For near UV CD, a 5 mm path length cuvette was used. Special care was taken to keep the loss in volume of the protein solution due to evaporation to less than 3% of the initial volume. The protein solutions were prepared in 5 mM acetate buffer (pH 3.0).

RESULTS

Hemolytic Activity. The hemolytic activity of CTX II and CTX IV monitored at various concentrations ranging from 2 to 20 μM shows that, at all concentrations of the toxins, the lytic activity of CTX IV was higher than that shown by CTX II (Figure 1). Interestingly, at 20 μM CTX concentration and after 15 min, CTX IV is found to lyse 25% of the total erythrocyte cells used in the experiment, whereas CTX II exhibits only 10% erythrocyte lytic activity in the same time period. The denatured and reduced samples of both CTX II and CTX IV did not exhibit any hemolytic activity (Figure 1), indicating that the enhanced lytic activity of CTX IV is due to some unique feature(s) in its three-dimensional structure.

Circular Dichroism. Comparison of the circular dichroism spectra of CTX II and CTX IV in the near-UV region shows

[1] Abbreviations: DQF-COSY, double quantum filtered correlated spectroscopy; NOE, nuclear Overhausser effect; NOESY, two-dimensional nuclear Overhauser enhancement spectroscopy; $^3J_{NH\alpha}$, vicinal spin−spin coupling constant between NH and α-proton; rmsd, root mean square deviation.

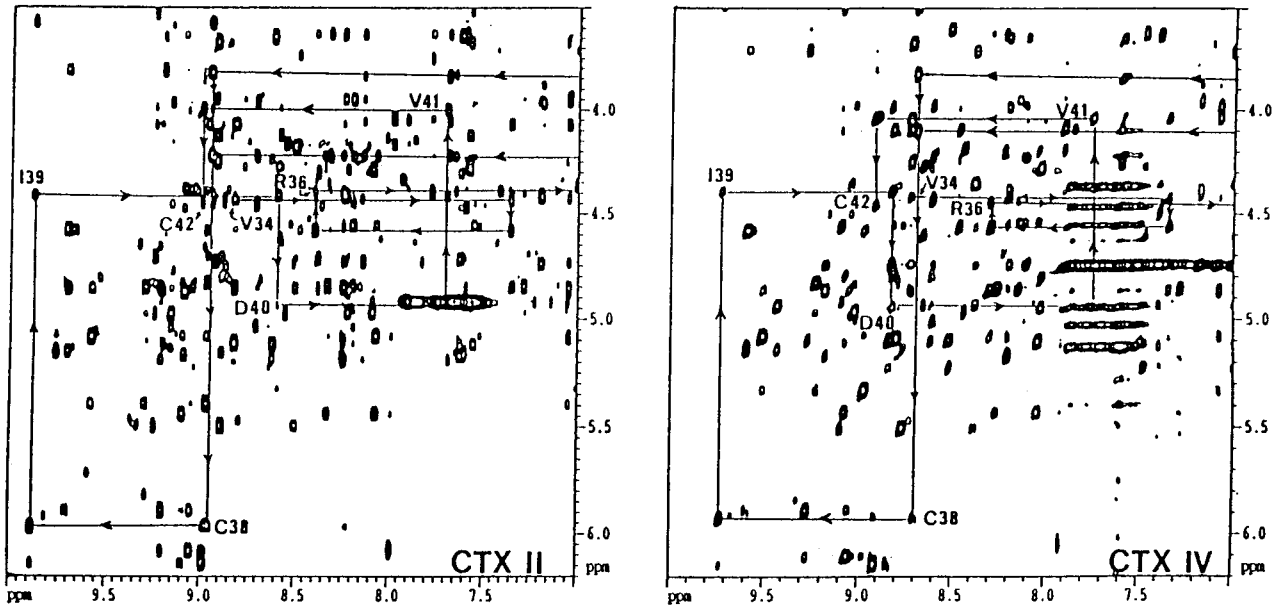

FIGURE 2: NOESY spectrum at 600 MHz (150 ms mixing period) of CTX II and CTX IV (pH 3.8), 20 °C in 90% H_2O/10% D_2O. Sequential $H^{\alpha}_{(i)}$-$NH_{(i+1)}$ connectivities between Val34 and Cys42 are indicated by connecting lines.

that both the toxins possess a broad CD band with a maximum centered around 270 nm (see Supporting Information). There are small differences in the intensities of the fine splittings in the near UV CD spectra indicating subtle variations in the microenvironment of the aromatic residues in both of these toxin isoforms. The CD spectra of CTX II and CTX IV in the far UV region (see Supporting Information) show positive ellipticity bands, one centered at 225 nm and the other band located at around 195 nm. The far UV CD spectra of these toxins also show a broad negative ellipticity band ranging from 208 to 218 nm (see Supporting Information). Presence of a negative CD band in this region of the spectra is indicative of the backbones of these two toxin analogues to be predominantly in the β-sheet conformation. The extreme of this negative ellipticity CD band in CTX II is located at 213 nm. While in CTX IV, the maximum of the negative CD band is blue-shifted to 210 nm.

ANS Emission. The emission spectra of ANS when bound to CTX IV and CTX II are different (see Supporting Information). The intensity emission when bound to CTX IV is at least 1.5 times greater than when bound to CTX II. The λ_{max} of ANS emission upon binding to CTX II is found to be 507 nm. The λ_{max} is blue-shifted by 2 nm (505 nm) when ANS is bound to CTX IV.

NMR Spectroscopy. Assignments of nearly all proton resonances in both the toxins (CTX II and CTX IV) were achieved using well-established sequence-specific methods (Wuthrich, 1986). The solution structure of CTX II was solved earlier by our research group (Bhaskaran *et al*., 1994c) at lower resolution using a 500 MHz NMR spectrometer. For a meaningful comparison with the solution structure of CTX IV, the structure of CTX II was recalculated using a 600 MHz spectrometer in the present study. As a consequence of better spectral resolution, minor errors in the earlier assignments (Bhaskaran et al., 1994c) of few resonances were observed. In both CTX II and CTX IV, the DQ-COSY (not shown) recorded in H_2O was of great value for unambiguous identification of glycine spin systems, since a remote peak is observed at $\omega_2 = \omega_{NH}$, $\omega_1 = \omega_2 + \omega_{\alpha 1}$. These peaks are located in a well-resolved region and thus were easily identified. Finally, the four proline residues in both toxins were successfully assigned from their J-connectivity network in the TOCSY and water-gated NOESY spectra (Figure 2).

A survey of the sequential NOE connectivities yielded the secondary structural information in both toxins (CTX II and CTX IV). Using the main-chain-directed (MCD) strategy (Englander & Wand, 1987), the secondary structure of both of these toxins was found to be primarily β-sheet. Thus, the two-dimensional NMR results fully corroborate with the CD results. In both CTX II and CTX IV, the residues existing in the β-sheet conformation are identical. The residues comprising the five β-strands which constitute the β-sheet segments include Lys2-Lys5 (strand I), Tyr11−Cys14 (strand II), Leu20−Phe25 (strand III), Val34−Ile39 (strand IV) and Lys50−Cys55 (strand V). Strands I and II constitute the antiparallel double-stranded β-sheet segment and the strands III, IV, and V comprise the β-stranded β-sheet. The hydrogen exchange data (see Supporting Information) on the two toxin isoforms (CTX II and CTX IV) reveal that 28 of the 60 amide protons are resistant to deuterium exchange in CTX IV. On the other hand, only 21 protons are protected from deuterium exchange in CTX II. Interestingly, the amino group of Arg1 and the amide proton of Cys3 are protected from exchange in CTX IV. In CTX II, a similar protection is not observed (see Supporting Information).

Structural Statistics. The CTX II and CTX IV structure calculations were performed based on a total of 560 and 580 distance constraints, respectively. In both CTX II and CTX IV, the overlap of the 12 simulated annealing structures were in good agreement with the NMR data (Figure 3). The backbone rmsd values for all heavy atoms in CTX II and CTX IV were 0.73 and 0.69 Å, respectively. Thus considering only the well-defined secondary structure regions, excluding the more disordered loops, the backbone rmsds in the both CTX II and CTX IV are in the range 0.3−0.4 Å. Convergence of the selected structures were also confirmed by the ϕ and ψ values and are found to be within their allowed regions (see Supporting Information).

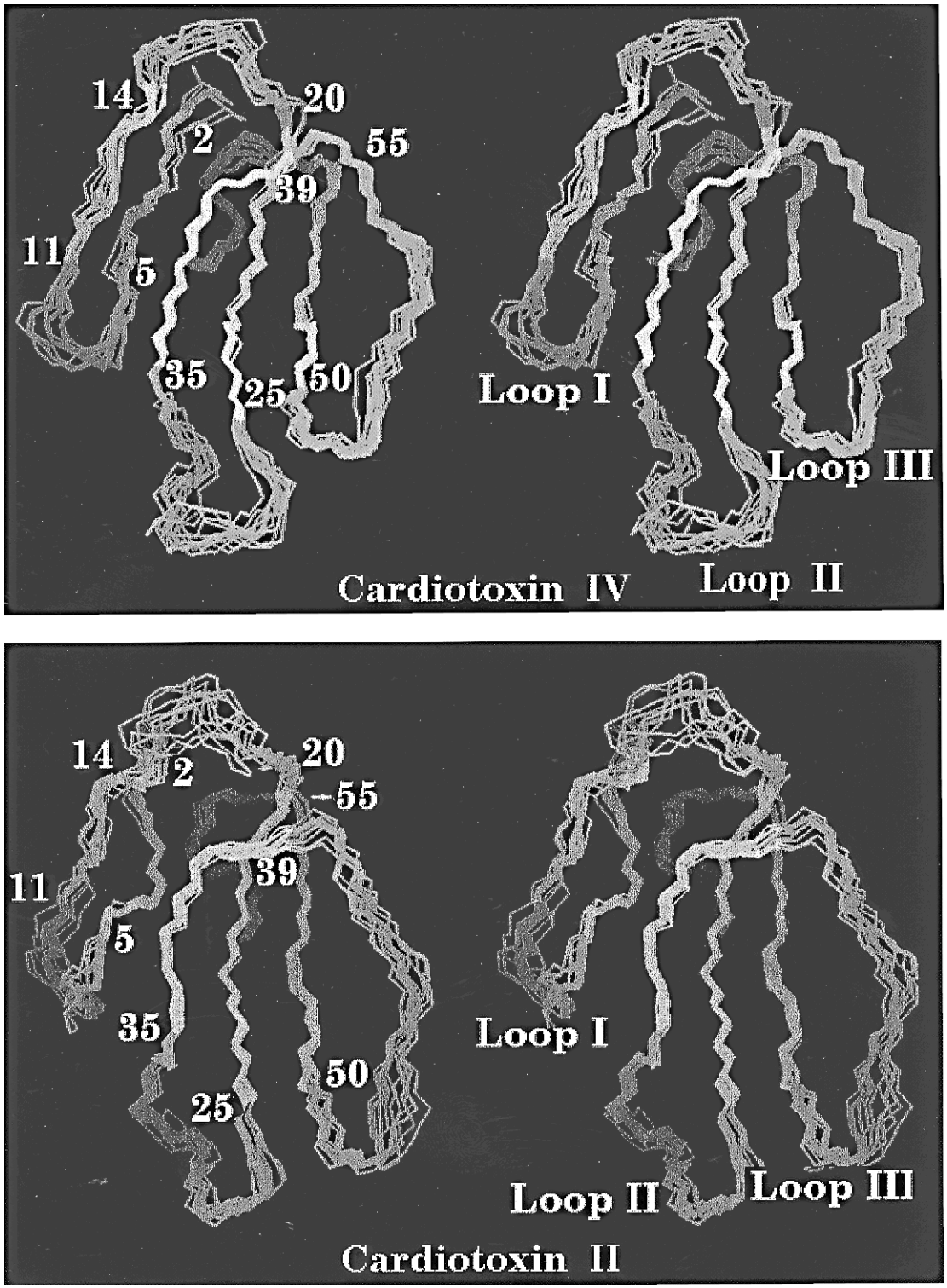

FIGURE 3: Stereoview of the best-fit superposition of the 12 NMR solution structures of CTX IV and CTX II as determined by dynamical simulated annealing calculations. The residue numbers indicate the location of each of the β-strands that make up the double-, and triple-stranded β-sheet segments in the toxin.

Thermal Stability. Figure 4 shows the thermal denaturation profiles of CTX II and CTX IV using the far- and near-UV CD spectra as a probe to monitor the unfolding of the toxin isoforms. The thermal unfolding monitored from the mean residue ellipticity changes at 213 nm essentially provides information regarding the melting of the secondary structures of these toxin analogues (CTX II and CTX IV). The heat-induced unfolding of both CTX II and CTX IV appear to be cooperative. However, the midpoints of thermal transitions (T_m) value of the two cardiotoxin analogues differ from each other significantly. The structure of CTX IV (T_m = 67 ± 0.3 °C) appears to be thermally more stable than that of CTX II (T_m = 64 ± 0.4 °C).

DISCUSSION

It is well-known that many isoforms of cardiotoxins exist in a single venom source. It is important to understand the structure−function relationships that could possibly exist among the various cardiotoxin isoforms. In this context, the present study is aimed at elucidating the differences in the

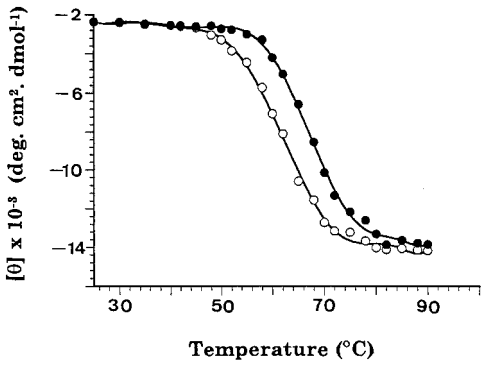

FIGURE 4: Thermal denaturation profiles of CTX II (open circles) and CTX IV (filled circles) in 10 mM acetate buffer (pH 3.0), monitored from the mean residue ellipticity changes at 213 nm using far UV circular dichroism. The midpoints of thermal transitions (T_m) of CTX II and CTX IV have been found to be 63 ± 0.4 °C and 67 ± 0.3 °C, respectively.

structure and biological activities of two cardiotoxin analogues, CTX II and CTX IV from the venom of *N. naja atra*.

The comparison of the solution structures of CTX II and CTX IV shows that the overall topologies of the structures of these two toxins are similar. The general architecture of CTX II and CTX IV comprises three loops protruding from a globular head (Figure 3). The secondary structural elements in both the toxin isoforms consists of five β-strands arranged in the form of antiparallel double- and triple-stranded β-sheets. The location and amino acids involved in the β-sheet segments are identical in both CTX II and CTX IV (Figure 3). The far-UV CD spectrum of these toxin isoforms also reveals their β-sheet conformation (see Supporting Information). In addition, both in CTX II and CTX IV, two well-defined type I β-turns are found. One of them is located between Ser46 and Val49, and the other is observed between Thr56 and Cys59.

The solution structures of CTX II and CTX IV show subtle but significant differences in the backbone folding. In CTX IV, interestingly, Val34 located in the triple-stranded β-sheet segment has ϕ and ψ angles of −133° and −52.5° ($<\phi> = -133° \pm 10°$ and $<\psi> = 52.5° \pm 15°$) (see Supporting Information), respectively. These values are close to those observed for a residue at position 1 in a β-bulge. This local structure appears to compensate the disruption of the regularity of the β-sheet due to the presence of proline at position 33. The bulge increases the twist of the triple stranded β-sheet. The β-bulge found in CTX IV, in principle, could be classified as a G1 type β-bulge according to the classification of Richardson (1981). Val34 is found to exist in a β-bulge in at least two other cardiotoxin analogues whose solution structures have been described (Gilquin *et al*., 1993; Jahnke *et al*., 1994). Interestingly, such a β-bulge is not found in CTX II. Val34 in CTX II has ϕ and ψ angles of −68° and −36°. Thus, it appears that the orientation of the strand IV (residues 34−39) is different in CTX II and CTX IV. Interestingly, the deviations in the chemical shift values of the amide protons of the residues involved in the strand IV in CTX II and CTX IV are significant.

The most important difference in the backbone folding of CTX IV and CTX II is found to occur at the N- and the C-terminal ends. The carboxyl end in CTX IV appears to be spatially close to the amino-terminal end as indicated by the presence of several NOEs. For example, the following NOEs could be noticed between the N- and C-terminal residues in CTX IV: Asn4NH−Cys59NH, Cys3H$^{\alpha}$−Arg58NH, and Asp57NH−Arg58H$^{\epsilon}$. The N- and the C-terminal ends in CTX IV appear to be connected *via* a salt-bridge between the side chain guanido and carboxylate groups of Arg1 and Asp57, respectively (Figure 5). This salt-bridge aids in bringing together the N- and C-terminal ends in CTX IV. In CTX II, this crucial salt-bridge does not exist (Figure 5). Interestingly, comparison of the amide proton-deuterium exchange data of both CTX II and CTX IV shows that the amide proton exchange pattern in the N- and C-terminal regions is significantly different in both the toxins. In CTX IV, the amide proton protection for the residues in the N- and C-terminal ends of the molecule are higher as compared to in CTX II (see Supporting Information). Interestingly, the N-terminal amino group is protected from exchange in CTX IV but not in CTX II. Thus, it appears that the structure of CTX IV is characterized by additional structural interactions [such as hydrogen bonding and salt bridge(s)] compared to the solution structure of CTX II, among the residues located at the N- and C-termini of the molecule. This aspect is supported by the evidence obtained from the thermal denaturation experiments (Figure 4), wherein the structure of CTX IV is found to be more stable than that of CTX II.

The three-dimensional solution structures of both CTX IV and CTX II are characterized by continous patches of hydrophobic residues at the surface of these toxin molecules. The tip of loop I is completely hydrophobic, and this hydrophobic stretch is flanked by basic residues such as lysine and arginine. There are subtle differences in the exposure of the residues in hydrophobic patch in loop I between CTX II and CTX IV. Comparison of the solution structures of CTX II and CTX IV shows that the side chains of Leu6, Val7, Leu9, and Phe 10 in CTX II are more exposed to the solvent than in CTX IV. This observation is supported by the chemical shift values of the amide protons of Val7 and Leu9 in CTX IV, which are shifted to higher field as compared to in CTX II. The increased intensity and the small blue-shift in the emission maximum of ANS bound to CTX IV also indicates greater exposure of the hydrophobic residues in CTX IV than in CTX II (see Supporting Information). Menez and co-workers (Menez *et al*., 1990; Gilquin *et al*., 1993) studying the structure−function relationship of a cardiotoxin analogue (toxin γ) from the spitting cobra *N. nigricollis* demonstrated that loop I has a crucial role in the cytotoxic activity of cardiotoxins. In addition to the hydrophobic patch located in loop I, there is yet another hydrophobic cluster both in CTX II and CTX IV spanning a large part of loops II and III. This cluster includes residues Leu20, Leu40, Met24, Tyr51, Tyr22, and Ile39.

There are three tyrosine residues in CTX II and CTX IV located at amino acid positions 11, 22, and 51. The hydrophobic patch around Tyr22 and Tyr51 on the convex side is flanked by a group of three cationic residues, i.e., Lys12, Lys18, and Lys35. Chemical modification of these invariant lysine residues renders the cardiotoxin biologically inactive (Kini *et al*., 1987; Kini & Evans, 1989a,b; Menez *et al*., 1990). The orientations of these lysine resiudes are almost similar in CTX II and CTX IV, and this aspect appears to be essential for the lytic activity of cardiotoxins.

Erythrocyte lytic activity is the most reliable and reproducible test for snake venom cardiotoxins (Kumar *et al*.,

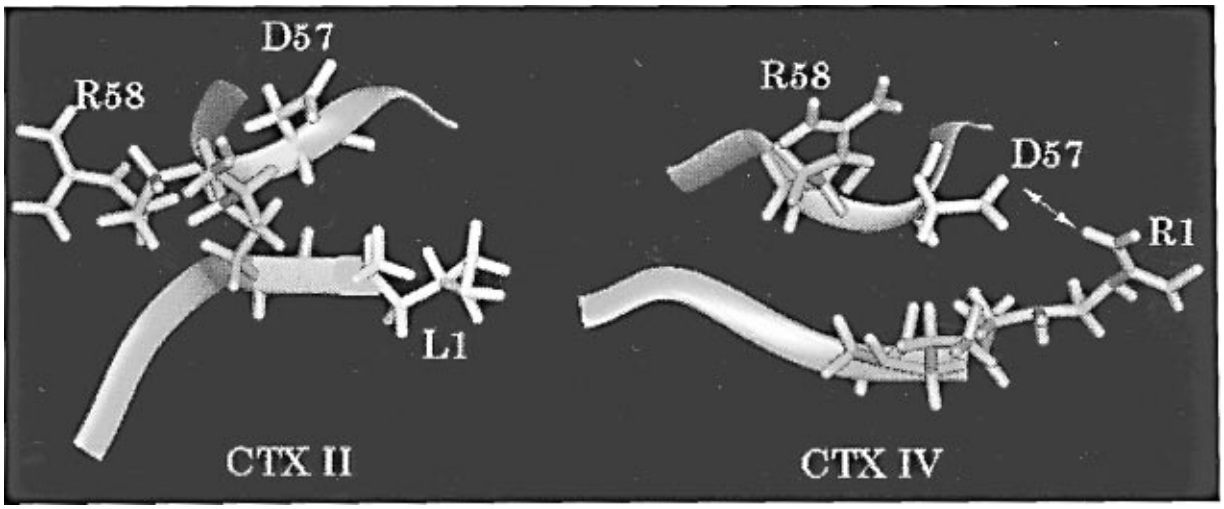

FIGURE 5: Depiction of the salt-bridge formation between the side chain groups of Arg1 and Asp57 in CTX IV. This salt-bridge locks the N- and C-terminal ends and is considered to be crucial for the development of the cationic cluster responsible for the enhanced erythroocyte lytic activity of CTX IV. There is no such salt-bridge in CTX II.

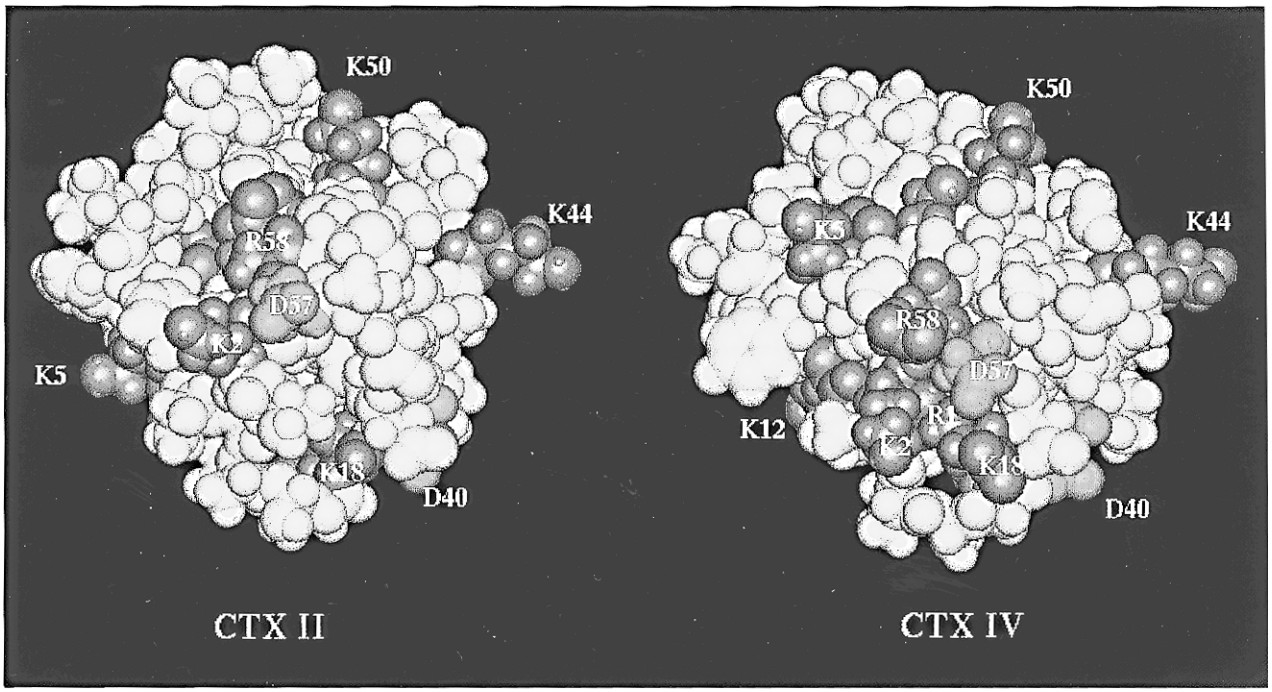

FIGURE 6: A top-view representation of the mean structure(s) of cardiotoxins indicating the surface charges in CTX II and CTX IV contributed by the various charged groups. The salt-bridge formed between the side chain guanido and carboxylate groups of Agr1 and Asp57 in CTX IV results in the formation of a "cationic cluster" comprising of residues Arg1, Lys2, Lys5, Lys12, Lys18, and Arg58. The positively charged residues (indicated in blue) in CTX II do not seem to organize into prominent cationic cluster(s).

1996a). Cardiotoxins have been shown to interact strongly with negatively charged phospholipid vesicles but not with neutral and positively charged vesicles (Faucon *et al*., 1993). Neutralization of positive charges by chemical modification is shown to result in substantial loss of lytic activity (Menez *et al*., 1990). The cationic centers on the cardiotoxin molecules are believed to facilitate binding of the toxin to the erythrocyte membrane through charge−charge interaction(s) (Batenburg *et al*., 1985; Dufton & Hider, 1991; Kumar *et al*., 1996a). Once anchored on the erythrocyte membrane, cardiotoxins are postulated to interact through the hydrophobic patches (on the toxin) with lipid surface on the erythrocyte membrane and induce phase separation (Batenburg *et al*., 1985) ultimately resulting in RBC lysis.

The crucial difference which could account for the difference in the hemolytic activities of CTX II and CTX IV is in the clustering patterns of the cationic residues in their three-dimensional structures. In CTX IV at the N-terminal end, there is a patch of positively charged residues in the concave side of the molecule. The guanido group of Arg1 is salt bridged to the carboxyl side chain of Asp57. Owing to this salt-bridge, a strong cluster of cationic residues inclusive of Arg1, Lys2, Lys5, Lys23, Arg36, and Arg58 is built (Figure 6). The cluster of positively charged residues at the N-terminal end flanks the hydrophobic patch comprising of residues at the tip of Loop I (Figure 6). This cationic cluster is "dense" and could be responsible for the increased hemolytic activity of CTX IV over CTX II. Chemical modification studies on cardiotoxin analogue I from *Naja nigricollis crawshawii* (Kini & Evans, 1989b) have demonstrated that the well-conserved residues at the N-terminal end, namely Lys2, Lys5, and Arg58 play an important role

in the lytic activity of cardiotoxins. Arg1 in CTX IV appears to intensify the positive charge in CTX IV at the N-terminal end. In CTX II, owing to the lack of this salt-bridge, a cationic cluster (similar to the one observed in three-dimensional structures of CTX IV) is not observed in CTX II (Figure 6), and this aspect could be a strong reason for the lytic activity of CTX II being less than that of CTX IV.

The distribution of hydrophobic and hydrophilic amino acids in the three-dimensional structures of cardiotoxins is considered to be unique (among cardiotoxins) and has been postulated to be crucial for their biological activity (Kini & Evans, 1989b; Menez *et al*., 1990). The orientations of the hydrophobic side chains in both toxins are almost similar with the exception of loop I. The hydrophobic residues in CTX IV appear to be more exposed to the solvent than in CTX II. This aspect could also help in potentiating the lytic action of CTX IV. However, we believe that it is the differential distribution of the cationic residues in CTX II and CTX IV could directly account for the differences in the erythrocyte lytic activities of these two toxin isoforms. In CTX IV, the well-organized positively charged clusters on the concave side of the molecule could provide strong and multiple binding sites on the erythrocyte membrane through electrostatic interactions, eventually leading to lysis of the cells. In contrast, lytic activity of CTX II is lower (than in CTX IV) probably due to the lack of such an organized cationic cluster in the concave side of the molecule. The exact mechanism by which the cationic residues in cardiotoxins act to promote erythrocyte lysis is still not clear. We have recently cloned one of the cardiotoxin analogues from the Taiwan Cobra (Kumar *et al*., 1996b), and work is underway using site-directed mutants to evaluate the role of cationic clusters in the lytic activity.

ACKNOWLEDGMENT

We acknowledge the Regional Instrumentation Center, Hsinchu, Taiwan, for allowing us to use the 600 MHz spectrometer facility.

SUPPORTING INFORMATION AVAILABLE

Complete ^{1}H resonance assignments for CTX II and CTX IV (Tables S1 and S2), far UV and near UV CD spectra of CTX II and CTX IV (Figure S1), emission spectra of ANS bound to CTX II and CTX IV (Figure S2), hydrogen-deuterium exchange pattern of CTX II and CTX IV (Figure S3) and ramachandran plots of the backbone conformational angles in the average structure of CTX II and CTX IV (Figure S4) (8 pages). Ordering information is given on any current masthead page.

REFERENCES

Batenburg, A. M., Bougis, P. E., Rochat, H., Verkleij, A. J., & de Kruijff, B. (1985) *Biochemistry 24*, 7101−7110.

Bax, A., & Davies, D. G. (1985) *J. Magn. Res. 65*, 355−360.

Bhaskaran, R., Yu, C., & Yang, C. C. (1994a) *J. Protein Chem. 13*, 503−504.

Bhaskaran, R., Huang, C. C., Chang, D. K., & Yu, C. (1994b) *J. Mol. Biol. 235*, 1291−1301.

Bhaskaran, R., Huang, C. C., Tsai, Y. C., Jayaraman, G., Chang. D. K., & Yu, C. (1994c) *J. Biol. Chem. 269*, 23500−23508.

Brackenridge, R., & Dufton, M. J. (1987) *J. Mol. Evol. 26*, 274−283.

Brünger, A. T. (1992) *X-PLOR software manual*, version 3.1, Yale University, New Haven, CT.

Chazin, W. J., Rance, M., & Wright, P. E. (1988) *J. Mol. Biol. 202*, 603−622.

Chiou, S. H., Huang, C. C., Huang, H. C., Chen, S. T., Wang, K. T., & Yang, C. C. (1995) *Biochem. Biophys. Res. Commun. 206*, 22−32.

Clore, G. M., Gronenborn, A. M., Brunger, A. T., & Karplus, M. (1985) *J. Mol. Biol. 186*, 435−455.

Driscoll, P. C., Gronenborn, A. M., Beress, L., & Clore, G. M. (1989) *Biochemistry 28*, 2188−2198.

Dufton, M. J., & Hider, R. C. (1991) in *Snake Toxins* (Harvey, A. L., Ed.) pp 259−302, Pergamon Press, New York.

Englander, S. W., & Wand, A. J. (1987) *Biochemistry 26*, 5963−5958.

Faucon, J. F., Dufourcq, J., Bernard, E., Duchesneau, L., & Pezolet, M. (1993) *Biochemistry 22*, 2179−2183.

Gilquin, B., Roumestand, C., Justin, Z. S., Menez, A., & Toma, F. (1993) *Biopolymers 33*, 1659−1675.

Hyberts, S. G., Marki, W., & Wagner, G. (1987) *Eur. J. Biochem. 164*, 625−635.

Jahnke, W., Mierke, D. F., Beress, L., & Kessler, H. (1994) *J. Mol. Biol. 240*, 445−458.

Jayaraman, G., Kumar, T. K. S., Arunkumar, A. I., & Yu, C. (1996) *Biochem. Biophys. Res. Commun. 222*, 33−37.

Kini, R. M., & Evans, H. J. (1989a) *Biochemistry 28*, 9209−9215.

Kini, R. M., & Evans, H. J. (1989b) *Int. J. Pep. Protein Res. 34*, 277−286.

Kini, R. M., Stefansson, S., & Evans, H. J. (1987) in *Progress in venom and Toxin research* (Gopalakrishnakone, P., & Tan, C. K. Eds.) pp 175−185, National University of Singapore, Singapore.

Kumar, T. K. S., Lee, C. S., & Yu, C. (1996a) in *Natural Toxins II* (Tu, A. T., & Singh, B. R. Eds.) pp 115−129, Plenum Press, New York.

Kumar, T. K. S., Yang, P. W., Lin, S. H., Wu, C. Y., Lei, B., Lo, S. J., Tu, S. C., & Yu, C. (1996b) *Biochem. Biophys. Res. Commun. 219*, 450−456.

Menez, A., Gatineau, E., Roumestand, C., Harvey, A. L., Mouawad, L., Gilquin, B., & Toma, F. (1990) *Biochemie 72*, 575−588.

Nilges, M., Clore, G. M., & Gronenborn, A. M. (1988) *FEBS Lett. 239*, 129−136.

O'Connell, J. F., Bougis, P. E., & Wuthrich, K. (1993) *Eur. J. Biochem. 213*, 891−900.

Pardi, A., Billitier, M., & Wuthrich, K. (1984) *J. Mol. Biol. 180*, 741−751.

Peng, S. S., Kumar, T. K. S., Jayaraman, G., Chang, C. C., & Yu, C. (1997) *J. Biol. Chem. 272*, 7817−7823.

Piotto, M., Saudek, V., & Skelnar, V. (1992) *J. Biomol. NMR 2*, 661−665.

Rance, M., Sorenson, O. W., Bodenhausen, G., Wagner, G., Ernst, R. R., & Wuthrich, K. (1983) *Biochem. Biophys. Res. Commun. 117*, 479−485.

Richardson, J. S. (1981) *Adv Protein Chem. 34*, 167−339.

Wagner, G., & Zuiderweg, G. R. P. (1983) *Biochem. Biophys. Res. Commun. 113*, 854−860.

Wagner, G., Braun, W., Havel, T. F., Schaumann, T., & Wuthrich, K. (1987) *J. Mol. Biol. 196*, 611−639.

Williamson, M. P., Havel, T. F., & Wuthrich, K. (1985) *J. Mol. Biol. 182*, 295−315.

Wuthrich, K. (1986) *NMR of proteins & nucleic acids*, John Wiley & Sons Inc., New York.

Wuthrich, K., Billitier, M., & Braun, W. (1983) *J. Mol. Biol. 169*, 949−961.

Yang, C. C., King, K., & Sun, T. P. (1981) *Toxicon 19*, 645−659.

Yu, C., Lee, C. S., Chaung, L. C. Shei, Y. R., & Wang, C. Y. (1990) *Eur. J. Biochem. 193*, 789−799.

Yu, C., Bhaskaran, R., Chaung, L. C., & Yang, C. C. (1993) *Biochemistry 32*, 2131−2136.

Yu, C., Bhaskaran, R., & Yang, C. C. (1994) *J. Toxin. Toxicol. Rev. 13*, 291−315.

BI971107A